Phase Locked Loop Control of Inverters in a Microgrid

Matthew Surprenant
Dept of ECE
University of Wisconsin
Madison, WI, USA

Ian Hiskens
Dept of EECS
University of Michigan
Ann Arbor, MI, USA

Giri Venkataramanan
Dept of ECE
University of Wisconsin
Madison, WI, USA

Abstract—**Microgrids are small-scale electricity supply networks that have local power generation. This paper considers a control strategy for inverter-based microsources within a microgrid. The general control philosophy within a microgrid is that sources must rely only on local information, yet must cooperate with other sources. To accomplish that goal, the proposed controller uses droop characteristics for active-power/frequency and reactive-power/voltage. The proposed control strategy is based on the use of a phase locked loop to measure the microgrid frequency at the inverter terminals, and to facilitate regulation of the inverter phase relative to the microgrid. This control strategy allows microgrids to seamlessly transition between grid-connected and autonomous operation, and vice versa. The controller has been implemented in an actual microgrid that incorporated multiple sources. The paper provides simulation results and documents the performance of the hardware implementation.**

I. INTRODUCTION

A microgrid is a small electric grid that delivers electricity to a building or a group of buildings [1], [2]. Microgrids are capable of both generating their own electric power with small-scale distributed generation (microsources) and receiving/exporting power to the main utility grid [3]. Microgrids represent a major departure from centralized power distribution systems.

There are basically two categories of microsources in a microgrid, inverter-based and synchronous generators. Inverter-based sources are those that do not generate power at the grid frequency, and thus need an inverter to interface with the microgrid [4], [5], [6]. Such sources include photovoltaic panels, fuel cells, wind power, microturbines, and batteries. Synchronous sources, such as diesel gensets, are currently more common, though inverter-based generation is steadily growing.

Microgrids offer improved reliability through their ability to island. Islanding means that the microgrid continues to operate autonomously when disconnected from the grid. Islanding provides microgrid customers with greater reliability because power can continue to be supplied when the utility system is interrupted. A microgrid is generally connected to the utility grid through a single connection point, so it is easily islanded by opening the circuit breaker at that point. After islanding, the
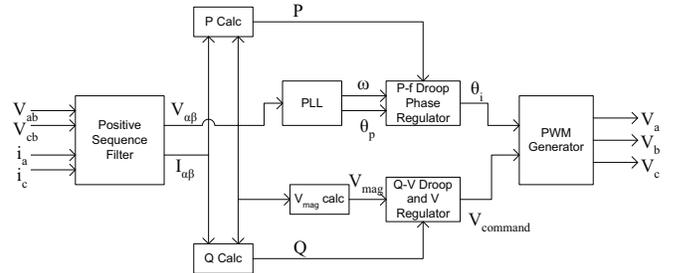
Fig. 1. Block diagram of inverter control.

microgrid should continue to serve its loads without disruption. The microgrid must also be able to resynchronize with the grid when the condition that initiated islanding has been corrected. This paper presents an inverter control scheme that achieves these islanding requirements.

The concept of "plug and play" microsources is key to microgrids. This simply means that power sources rely only on information that is locally available at their network terminals, and hence there is no need for communications between sources. This keeps microgrid systems simpler, and implies that customized engineering should not be required for each microsource. Rather, a microsource should be able to be added to a microgrid and operate correctly without special design. To accomplish this goal, the ideas of active-power/frequency and reactive-power/voltage droop controls have been used. They allow microsources to share power and maintain stability without the need for fast communications.

The paper is organized as follows. Section II provides an overview of the inverter control scheme, including a discussion of the phase-locked loop implementation and regulator design. Simulation results are presented in Section III. Section IV describes an actual microgrid that was built to test the controller, and presents experimental results. Conclusions are provided in Section V.

II. INVERTER CONTROL SCHEME

A. Overview

The control scheme for the microsource inverter is based on a phase-locked loop (PLL) for frequency and phase detection, together with conventional microgrid active-power/frequency
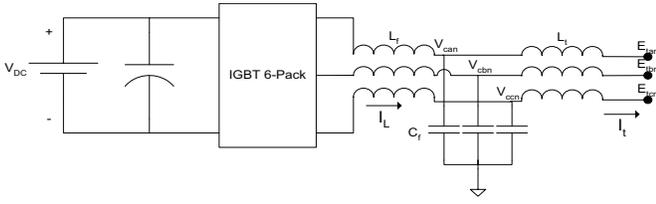
Fig. 2. Inverter circuit diagram.

TABLE I
INVERTER FILTER PARAMETERS.

Component	Value
L_f	0.97 mH
C_f	30 μF
L_t	5.0 mH

and reactive-power/voltage droops. The block diagram of the entire control strategy is shown in Figure 1. The initial step in the control algorithm is to transform phase voltages and currents into stationary reference frame (α and β) quantities. The α- and β-voltage components are used by the PLL to estimate the frequency and establish the phase reference for the inverter. These quantities are provided to the phase regulator which computes the desired output phase of the inverter. The voltage regulator computes and regulates the desired voltage magnitude of the inverter. Lastly, the PWM generator takes the desired voltage magnitude and phase and creates the PWM output signals.

B. Inverter characteristics

Each inverter in the microgrid is set up in accordance with the circuit shown in Figure 2. The DC bus was powered by a DC supply operating at 750 V_{DC}. An IGBT six pack was used for switching. On the AC side, an LCL filter was used to attenuate the switching frequency and smooth the AC waveform. The filter parameters are given in Table I. The output of the filter was connected to the microgrid through a Y-Δ transformer which stepped the voltage down from 480 V to 208 V. The controller used voltage measurements $E_{t,ab}$ and $E_{t,cb}$, and current measurements $I_{t,a}$ and $I_{t,c}$.

C. Three-phase PLL design

A block diagram displaying the functional components of a generic PLL is shown in Figure 3. For small deviations, standard simplifying assumptions [7] allow the PLL to be modeled according to the linear block diagram of Figure 4, where δ_t is the phase of the measured voltage and δ_p is the phase estimate given by the PLL. In order to establish the PLL error signal $\delta_t - \delta_p$ for phase tracking in a three-phase system, we have adopted an approach suggested by [6], [8].

The first step in this process is to express the measured three-phase voltages in the stationary reference frame. This is achieved through the transformation,

$$\begin{bmatrix} V_\alpha \\ V_\beta \end{bmatrix} = \frac{2}{3} \begin{bmatrix} 1 & -\frac{1}{2} & -\frac{1}{2} \\ 0 & -\frac{\sqrt{3}}{2} & \frac{\sqrt{3}}{2} \end{bmatrix} \begin{bmatrix} V_a \\ V_b \\ V_c \end{bmatrix}. \tag{1}$$
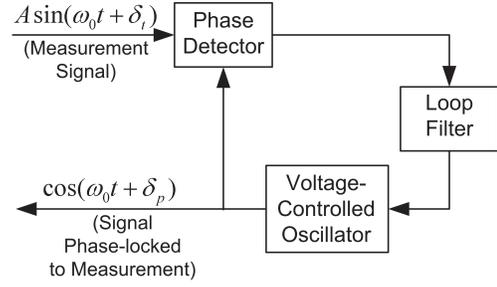

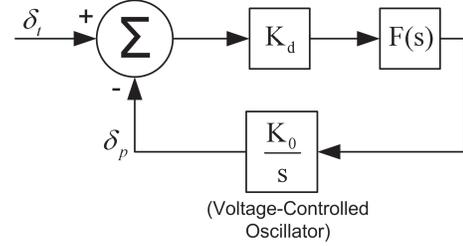Fig. 3. Generic PLL block diagram.

Fig. 4. Linearized PLL block diagram.

The stationary reference frame voltages V_α and V_β are then transformed into the synchronous reference frame, according to,

$$\begin{bmatrix} V_q \\ V_d \end{bmatrix} = \begin{bmatrix} \cos \delta_p & -\sin \delta_p \\ \sin \delta_p & \cos \delta_p \end{bmatrix} \begin{bmatrix} V_\alpha \\ V_\beta \end{bmatrix} \tag{2}$$

where δ_p is the estimate of the phase given by the PLL. It can be shown that

$$V_d = -V_t \sin(\delta_t - \delta_p) \tag{3}$$

where V_t is the magnitude of the measured AC voltage. Assuming $(\delta_t - \delta_p)$ is small, (3) can be approximated by

$$V_d = -V_t(\delta_t - \delta_p). \tag{4}$$

It follows that the goal of the PLL is to drive $-V_d$ to zero. This can be achieved with good performance by using a proportional-integral (PI) controller for the loop filter,

$$F(s) = K_p + \frac{K_i}{s}. \tag{5}$$

Defining

$$\dot{\delta}_p = \omega_p \tag{6}$$

and manipulating the equations associated with the PLL gives,

$$\dot{x} = K_3(\delta_t - \delta_p) \tag{7}$$
$$\omega_p = K_4(\delta_t - \delta_p) + x \tag{8}$$

where $K_3 = K_d K_i K_o$ and $K_4 = K_d K_p K_o$.

D. Regulation

The control objectives are to regulate the terminal bus voltage magnitude V_t, and the active power delivered to the grid P_{gen}. The first objective can be achieved by simple integral control

$$\dot{m} = K_1(V_{set} - V_t) \tag{9}$$

where m is the inverter modulation index. The voltage setpoint V_{set} may be constant, or may follow a droop characteristic that is dependent upon the reactive power delivered to the grid.

The phase of the inverter voltage is regulated to control the active power output of the inverter. The basic idea behind this strategy is proposed in [4]. The inverter interface with the microgrid can be modeled according to

$$P_{gen} = \frac{V_i V_t}{X} \sin(\delta_i - \delta_t) \tag{10}$$

where $V_i \angle \delta_i$ is the voltage synthesized at the inverter bus, $V_t \angle \delta_t$ is the voltage on the grid side of the filter, and jX is the effective impedance between those two points. Assuming V_i and V_t remain relatively constant, regulation of P_{gen} can be achieved by controlling the angle difference $\delta_i - \delta_t$. The PLL output δ_p provides a filtered version of δ_t though, so it is preferable to control

$$\theta = \delta_i - \delta_p. \tag{11}$$

Integral control gives,

$$\dot{\theta} = K_2(P_{set} - P_{gen}). \tag{12}$$

The active power setpoint P_{set} is usually dependent upon a droop characteristic of the form

$$P_{set} = P^0 - R\omega_p, \tag{13}$$

where P^0 is the nominal power output of the microsource, ω_p is the estimated frequency deviation provided by the PLL, see (6), and R is the droop constant. The droop constant is determined so that at maximum power output the frequency will be at its minimum allowable value, and that at minimum power, the frequency will be at its maximum value.

Bringing the complete control strategy together gives,

$$\dot{m} = K_1(V_{set} - V_t)$$
$$\dot{\theta} = K_2(P_{set} - P_{gen})$$
$$\dot{x} = K_3(\delta_t - \delta_p)$$
$$\dot{\delta}_p = \omega_p$$
$$0 = P_{set} - (P^0 - R\omega_p)$$
$$0 = \theta - (\delta_i - \delta_p)$$
$$0 = \omega_p - (K_4(\delta_t - \delta_p) + x).$$

The PLL and power regulator are described by the block diagram of Figure 5.

III. SIMULATION RESULTS

The microgrid shown in Figure 6 will initially be used to illustrate the dynamic behaviour of the inverter control scheme. Inverter-based sources are located at buses 2 and 3, and a constant power load is connected to bus 4. Bus 1 forms the interface between the microgrid and the rest of the power system, which is modeled as an infinite bus. All of the AC quantities are expressed as per-unit values using a power base of 100 kVA.

For this example, both inverters have the parameters given in Table II. Plant 1 has a power setpoint of 0.7 pu (70 kW),
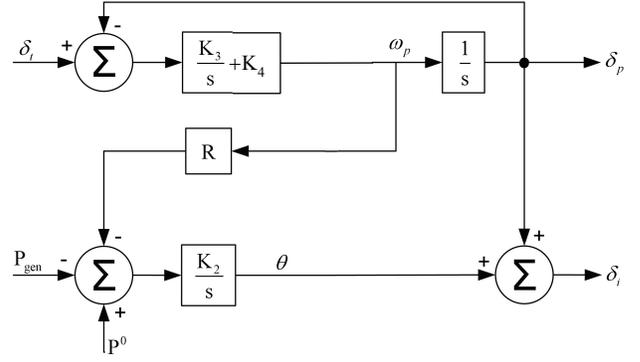
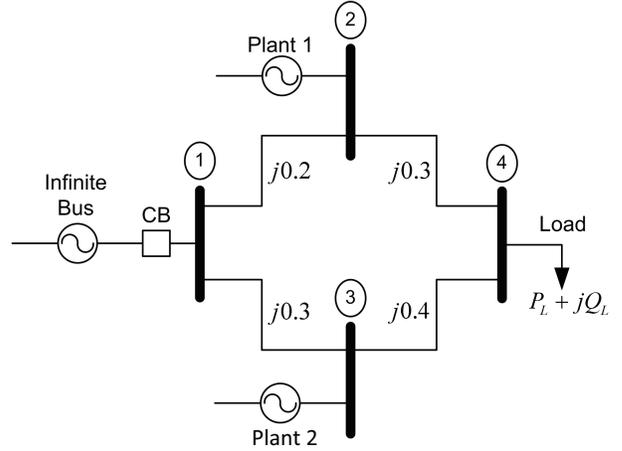Fig. 5.   PLL and active power regulation block diagram.

Fig. 6.   Microgrid layout for simulation example.

and Plant 2 has a power setpoint of 0.6 pu (60 kW). The active and reactive power of the load, P_L and Q_L, are 1.7 pu and 0.6 pu, respectively, and the voltage of the infinite bus is set to 1 pu. The circuit breaker (CB) connecting bus 1 to the rest of the grid is initially closed. The two inverter-based plants together supply 1.3 pu of the active power demanded by the load. The remaining 0.4 pu active power is drawn from the main grid through bus 1. At 1 s, the CB opens. The constant load must now be supplied by the inverters. At 7 s, the CB is signaled to close, but closing is prevented until the voltage magnitude appearing across the CB contacts reduces to a given threshold. For this simulation, the threshold is set to 0.22 pu. Consequently, the CB actually closes at 13.01 s.

Figure 7 shows the power delivered by each of the inverters over the simulation period, and Figure 8 shows the frequency deviation given by the inverter PLLs. When the microgrid is initially disconnected from the main grid, the power supplied from the DC bus immediately increases to compensate for the lost grid supply. Microgrid frequency drops in accordance with the droop characteristic. Note that Plant 1, which has a higher power setpoint, overshoots when the CB opens, while Plant 2 does not. The sum of the two power outputs must always equal the active power of the load while the CB is open.

When the CB recloses, the phase relationship between the

parameter	value
K_1	10
K_2	20
K_3	20
K_4	10
R	0.4
X	0.2pu
V_{set}	1pu
V_{dc}^{set}	480V

Fig. 7.   Power output of the inverters.

Fig. 8.   PLL frequency deviation of inverters.
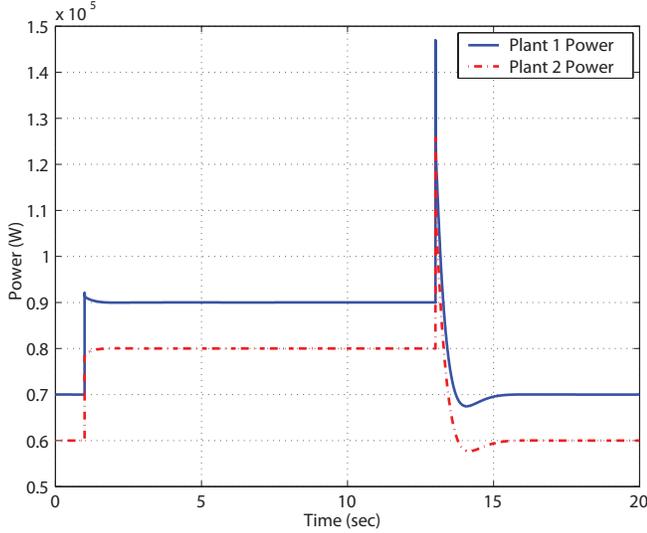

Fig. 9.   Plant 1 inverter angle behaviour relative to a global reference.

inverter voltages (which cannot change instantaneously) and the grid is such that active power initially flows from the microgrid to the infinite bus. Therefore, both plants see a power spike immediately following the reconnection. The inverter controls respond accordingly, with active power outputs quickly returned to their pre-disturbance values, and microgrid frequency restored to the nominal value.

Note that the grid model uses a phasor representation for voltages and currents, and therefore does not provide an accurate representation of fast transient behaviour [9]. In reality, the transformer inductance would limit the rate of change of the inverter current, so the spike would be smaller than indicated in Figure 7.

Figure 9 shows angle behaviour during the disturbance. (Only Plant 1 inverter quantities are shown.) When the CB opens, the inverter terminal bus voltage undergoes an immediate phase shift. Over the subsequent period of autonomous operation, the microgrid frequency is below nominal. Accordingly, the microgrid phase angle, relative to a global reference at nominal frequency, displays a steady decrease. This continues until the CB recloses. At that instant, the microgrid voltages are out of phase with the stronger system. In response, the inverter terminal bus phase angle adjusts very rapidly, quickly settling to a value that lags its initial value by exactly 2π radians.
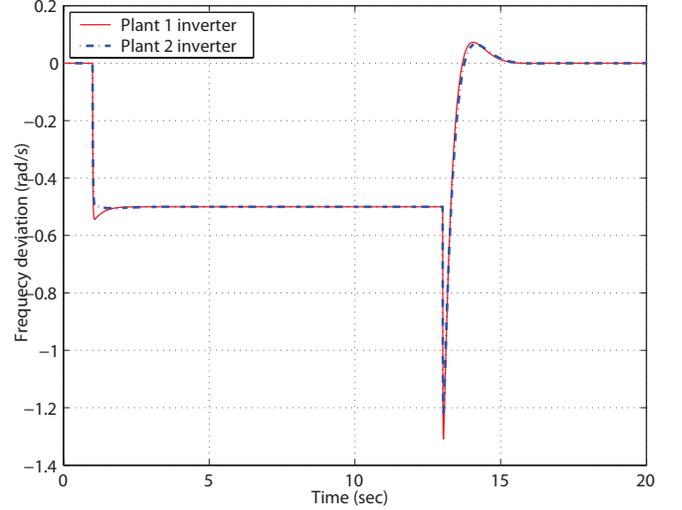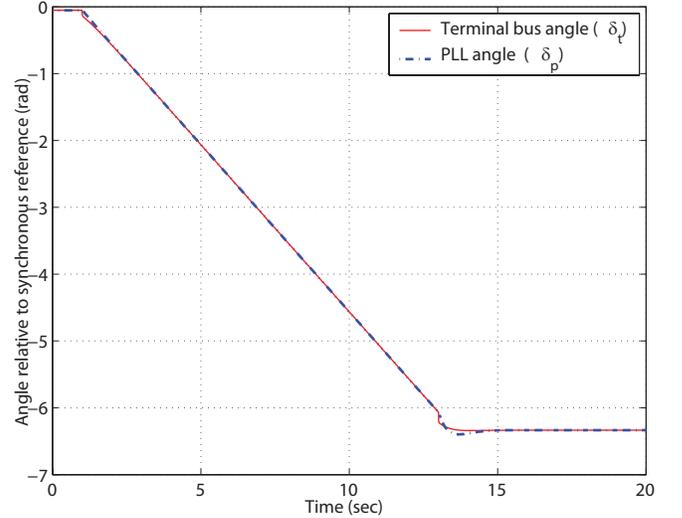
Figure 9 also shows that the PLL angle closely tracks the terminal bus angle. The difference between these quantities is shown more clearly in Figure 10. It can be seen that the controller is effective in rapidly driving this difference to zero. The angle difference across the inverter transformer is also shown in Figure 10. Notice that when the CB closes, the resulting phase shift in the inverter terminal bus voltage causes a spike in the angle difference across the inverter transformer. That spike in angle difference underlies the spike in active power P_{gen} observed in Figure 7.

IV. EXPERIMENTAL RESULTS

The PLL-based inverter control scheme was tested extensively using the radial microgrid shown in Figure 11. Initial testing used EMTP to simulate the response of the microgrid over a wide range of conditions. Those investigations confirmed the characteristics of the control algorithm, and assisted
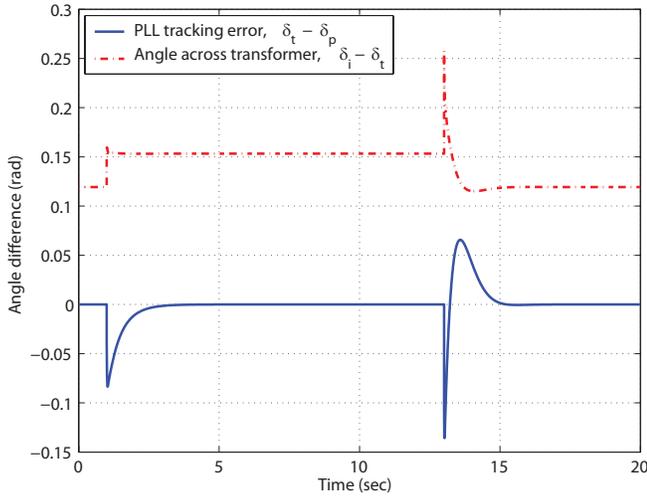
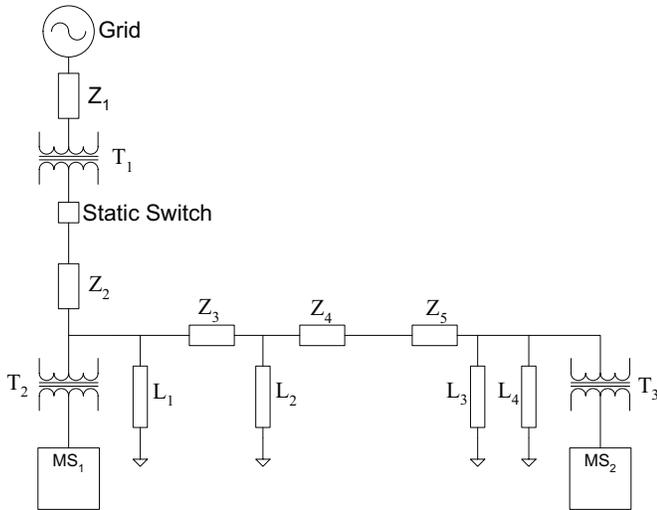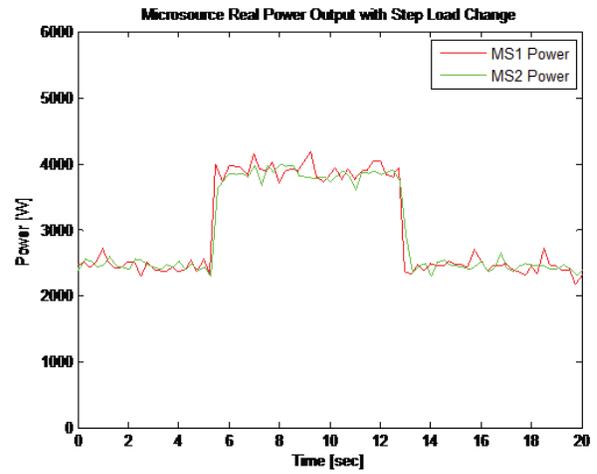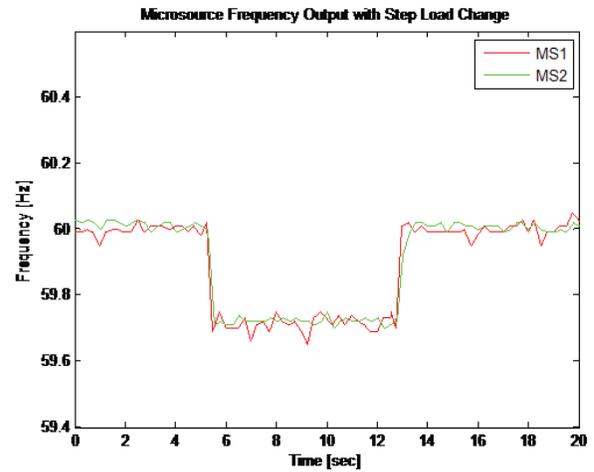Fig. 10.   Plant 1 inverter angle differences.

(a) Active power output.

Fig. 11.   Single line diagram of experimental microgrid.

(b) Microgrid frequency.

Fig. 12.   Microgrid behaviour for a step change in load.

in the tuning of controller parameters. The testing also provided confirmation that multiple inverter-based sources would interact appropriately when grid connected, when operating as an autonomous microgrid, and during transitions between those two states.

The microgrid of Figure 11 was implemented in hardware, in order to fully test the capabilities of the new control scheme. The PLL-based controller was implemented in a Freescale MPC555 microprocessor. The MPC555 is a 32-bit floating point processor. For the inverter control, the chip was over-clocked to run at 56 MHz. Also, due to time constraints on processor operations, most of the operations were carried out in fixed point. The trigonometric functions, sine and cosine, were calculated using lookup tables and interpolation. The switching frequency used was 10 kHz. The MPC555 has two A/D converters and samples the four signals once during each switching period. It outputs space vector pulse width modulation signals to the gate driver.

A number of experiments were undertaken. The first involved the two inverter-based sources operating in islanded mode. The load on the microgrid was stepped from 4.8 kW to 7.8 kW, and then back to 4.8 kW. The active power outputs of the two sources are shown in Figure 12(a). Both inverters share the load equally, both before and during the load step. The frequencies seen by the PLLs of the two inverters are shown in Figure 12(b). The frequency decline during the load step is a consequence of the droop characteristic.

For the second experiment, the microgrid was initially islanded from the utility grid. During the test, the microgrid was connected to the grid and subsequently islanded again. The active power outputs of the microsources and the injection from the grid are shown in Figure 13(a). The frequencies seen by the PLLs of the two inverters are shown in Figure 13(b). The active power setpoints for the two sources were set so that the microgrid frequency was initially below that of the grid. Upon connection to the grid, the microgrid frequency
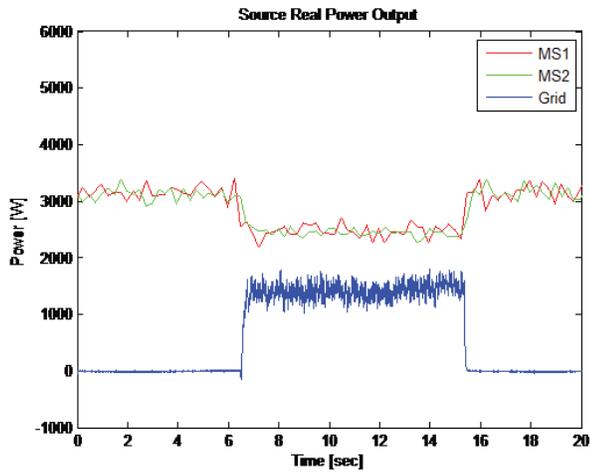
(a) Active power output.
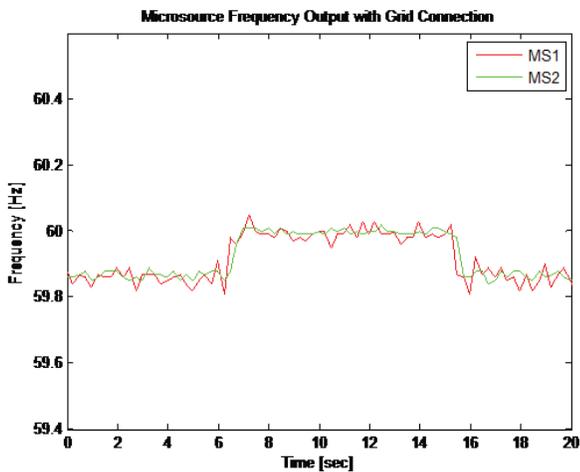
(b) Microgrid frequency.

Fig. 13.   Microgrid behaviour for grid connection and subsequent disconnection.

increased to match the grid, so the active power outputs of the two sources dropped in accordance with their droop characteristics. The resulting power mismatch was provided by the grid.

V. Conclusions

Many distributed generation sources, such as fuel cells and photovoltaic panels, cannot be connected directly to AC power systems. A power electronic interface is required, with a common topology consisting of a DC-AC voltage-source inverter. The paper has proposed an inverter control strategy that allows autonomous microgrids to be supplied solely by inverter-based sources.

The inverter controls regulate the power delivered to the grid, the terminal voltage, and also maintain the microgrid frequency. The proposed control scheme uses a phase-locked loop (PLL) to establish the microgrid frequency at the inverter terminals, and to provide a phase reference that is local to the inverter.

The proposed controller has been tested extensively in simulation and hardware. The controller allows sources to share active power generation without explicit communications, both in autonomous operation and when grid connected.

References

[1] R. Lasseter, "Microgrids," in *Proceedings of the IEEE Power Engineering Society Winter Meeting*, New York, NY, January 2002, pp. 305–308.

[2] P. Piagi and R. Lasseter, "Autonomous control of microgrids," in *Proceedings of the IEEE Power Engineering Society General Meeting*, Montreal, Quebec, June 2006.

[3] F. Katiraei and M. Iravani, "Power management strategies for a microgrid with multiple distributed generation units," *IEEE Transactions on Power Systems*, vol. 21, no. 4, pp. 1821–1831, November 2006.

[4] I. Hiskens and E. Fleming, "Control of inverter-connected sources in autonomous microgrids," in *Proceedings of the 2008 American Control Conference*, Seattle, WA, June 2008, pp. 586–590.

[5] K. Jaehong, J. Lee, and N. Kwanghee, "Inverter-based local AC bus voltage utilizing two DOF control," *IEEE Transactions on Power Electronics*, vol. 23, no. 3, pp. 1288–1298, May 2008.

[6] S.-K. Chung, "A phase tracking system for three phase utility interface inverters," *IEEE Transactions on Power Electronics*, vol. 15, no. 3, pp. 431–438, May 2000.

[7] D. Abramovitch, "Phase-locked loops: a control centric tutorial," in *Proceedings of the American Control Conference*, Anchorage, AK, May 2002.

[8] L. Arruda, S. Silva, and B. Filho, "PLL structures for utility connected systems," in *Proceedings of the IEEE Industry Applications Conference*, Chicago, IL, September 2001, pp. 2655–2660.

[9] P. Sauer, B. Lesieutre, and M. Pai, "Transient algebraic circuits for power system dynamic modeling," *International Journal of Electrical Power and Energy Systems*, vol. 15, no. 5, pp. 315–321, 1993.